Journal of Materials Chemistry A

ROYAL SOCIETY OF CHEMISTRY

PAPER

View Article Online
View Journal | View Issue

Cite this: J. Mater. Chem. A, 2024, 12, 30906

Room-temperature thermochemical water splitting: efficient mechanocatalytic hydrogen production†

Takuya Yamamoto, ‡[a] Sho Ashida, [b] Nanami Inubuse, [a] Shintaro Shimizu,[b] Yui Miura,[b] Tomoya Mizutani [b] and Ken-ichi Saitow ‡*[abc]

Received 5th July 2024
Accepted 1st October 2024

DOI: 10.1039/d4ta04650a

rsc.li/materials-a

Considering climate change and the environmental pollution crisis, CO_2-emission-free H_2 production based on green, low-energy processes is critically important. In this article, we report the accidental discovery and subsequent investigation of room-temperature thermochemical water splitting in a planetary ball mill. H_2 yields of ~20–1600% were obtained by milling six metals (Al, Zn, Fe, Ti, Mn, and Sn) and their oxides in water at 30–38 °C. Remarkably, when Ti was milled, H_2 was generated continuously until the water was consumed. Experimental and theoretical investigations—based on redox potentials, Gibbs energies, collision energies, and local temperatures and pressures—revealed that the milling medium acts as a mechano-cocatalyst, regenerating the catalyst (Ti and/or titanium oxides). Thus, thermochemical water splitting, *via* a cyclic mechanocatalytic TiO_2/Ti–water reaction, was responsible for the continuous H_2 production. The high H_2-production rate was attributed to reactions occurring in supercritical water at impact sites between balls, where the instantaneous local pressure and temperature were 11 GPa and 1300 °C, respectively. The production of high-purity hydrogen (>99%) using seawater feedstocks in a compact (~50 cm), low-power (~0.26 kW) reactor indicates that on-site, on-demand H_2 production is achievable.

Introduction

Sea and fresh water can be considered effective and abundant hydrogen atom reservoirs. In contrast, molecular hydrogen (H_2) is rare on Earth because it is released into outer space owing to its light weight. Consequently, most of the H_2 (95%) supplied to modern society is synthesized from fossil fuels *via* steam methane reforming ($CH_4 + 2H_2O \rightarrow CO_2 + 4H_2$).[1–3] Although relatively inexpensive, this method produces H_2 as well as large amounts of CO_2, consumes large quantities of thermal energy, and the reaction proceeds at high temperatures (650–1000 °C). Hence, alternative methods[1–3]—based on electrolysis,[4,5] electrocatalysis,[6,7] thermochemical water splitting,[8–10] photocatalytic water splitting,[11] biomass,[12,13] and chemical looping[14–16]—are actively being explored. However, real-world H_2-production methods must be cost-effective, efficient, and resilient to feedstock supply fluctuation. In addition, they should not produce CO_2, should possess all-weather functionality, and the H_2-production apparatus must be compact, stable, and durable.

Knowledge of metal–water reactions dates back centuries, with initial studies by Cavendish and Lavoisier having been reported in the 18th century. Extensive research starting in the 1980s revealed that H_2 can be synthesized at ~100% yield using Al or Mg alloys.[17–20] Thus, H_2 synthesis can be achieved using easily acquired materials and straightforward procedures, for example, by placing water and the alloy in a reaction vessel. In addition, metal–water reactions have other advantages, including no CO_2 emissions and low operating temperatures (25–80 °C). Furthermore, low-grade water (*e.g.*, sea, rain, and river water) can be used as H_2 feedstocks. However, metal–water reactions have the following disadvantages: first, oxide layers form on metal surfaces, hindering H_2 production; second, for real-world implementation, post-processing the metal oxide byproducts is critical; and third, continuous H_2 production is difficult because the metal reactant is consumed by the reaction.

These three drawbacks have been addressed by various researchers. Passivation layers can be removed, by alloying[17,18] or by using an alkali[19,20] or additives,[20] to deliver H_2 yields of 100%. Byproducts can also be converted into valuable products;

[a]Department of Chemistry, Graduate School of Science, Hiroshima University, 1-3-1 Kagamiyama, Higashi-Hiroshima, Hiroshima 739-8526, Japan. E-mail: saitow@hiroshima-u.ac.jp; Tel: +81-82-424-7487

[b]Department of Chemistry, Graduate School of Advanced Science and Engineering, Hiroshima University, 1-3-1 Kagamiyama, Higashi-Hiroshima, Hiroshima 739-8526, Japan

[c]Department of Materials Science, Natural Science Center for Basic Research and Development (N-BARD), Hiroshima University, 1-3-1 Kagamiyama, Higashi-Hiroshima, Hiroshima 739-8526, Japan

† Electronic supplementary information (ESI) available. See DOI: https://doi.org/10.1039/d4ta04650a

‡ These authors contributed equally to this work.

for example, $Al(OH)_3$ from the Al–water reaction is a feedstock for the manufacture of ceramics, medicines, and paper.[19,20] In addition, byproduct metal oxides can be recycled to produce H_2 by means of thermochemical water splitting.[8–10,14,15] However, although continuous H_2 production can be realized by thermochemical water splitting, the water-splitting temperature is typically so high (>2200 °C) that specific facilities, such as a nuclear reactor or large parabolic solar concentrator, are required.[1,3,8] Relatively low-temperature H_2-production processes—for example, the redox reactions of Mn(II)/Mn(III) oxides, occurring at 850 °C (ref. 9)—have been reported. Moreover, thermochemical cycles[3,8–10] or chemical loops[14–16] can split water at lower temperatures (500–1800 °C); however, the former involves the use of many chemicals and the creation of intermediates that decompose *via* multistep sub-reactions, while the latter either generates H_2 highly efficiently along with CO_2 or poorly without CO_2.

As an alternative method, mechanochemistry involves harnessing mechanical energy to drive chemical reactions.[21] It also encompasses chemical reactions that occur owing to the generation of localized heat and high pressure during impact when balls collide in a mechanochemical ball mill.[22–25] Indeed, instantaneous temperatures of ~1500 K and pressures of ~10 GPa upon collision can result in solid polymorph transformation, similar to the formation of natural polymorphs during meteorite impact and the generation of a crater on the Earth's surface.[26] Although mechanochemistry was identified by the International Union of Pure and Applied Chemistry (IUPAC) as one of the top 10 world-changing technologies in 2019,[21] the potential of this field of research in terms of applications to synthesis has yet to be fully explored. An early study revealed that magnetically stirring metal oxides in a glass vessel containing water produced small amounts of H_2.[27] In addition, H_2 generation has been triggered in water by milling quartz powder[28] and by the friction between milling balls and a vessel.[29] However, the very small amounts of generated hydrogen in these types of experiments mean that their applicability is limited.

Herein, we report the demonstration of Ti–water reactions in a planetary ball mill that produce H_2 in a highly efficient manner. It was observed that cyclic redox reactions continuously produced H_2 at temperatures close to room temperature until all the water was consumed. We accidently discovered this room-temperature thermochemical water splitting reaction while performing entirely different experiments, during the synthesis of nanoparticles by milling in water. Indeed, the H_2 pressure generated in the vessel during some of those experiments was so high that the seal of the vessel was broken and the vessel cover was blown to the laboratory ceiling. Thus, we changed the focus of our research from nanoparticle synthesis to H_2 production under controlled conditions using a planetary ball mill. In this article, we present the details of the reactions and their mechanisms.

Experimental

Mechanochemical reactions

A commercially available planetary ball-milling apparatus (Premium line P-7, Fritsch Japan Co., Ltd.) was employed for the mechanochemical metal–water reactions.[22,23,30–34] Either tungsten carbide (WC), stainless steel (SUS), or zirconia (ZrO_2) milling balls were used in vessels made of the same material to grind metal powders. The volume of the milling vessel was 80 mL in the absence of the water, metal powder, and balls. The diameters of the WC milling balls and total weight of the balls were 1.6 mm and 100 g, respectively; this weight corresponds to approximately 3000 balls; for the other milling media (SUS and ZrO_2), the experimental details are presented in Table S7 and Note S15 in the ESI.† Distilled water (10 mL, 0.56 mol) and metal powder (2 mmol) were placed in the vessel with the milling balls. The sizes of the particles in each of the metal powders were in the range of 5–100 μm. The vessel was purged with Ar prior to each milling process.

The milling balls in the vessel crushed the metal powders in water (100–700 rpm; revolution velocity : rotation velocity = −1 : 2), and a mechanochemical reaction between the water and metal powder was triggered by the action of the ball mill. The temperature T and pressure p of the gas in the milling vessel were tracked *in situ*, with measurements acquired every second during milling, using a thermometer and pressure sensor attached to the vessel cover (EASY-GTM, Fritsch Japan Co., Ltd.). The measured pressure $p(T, t)$ and temperature T of the gas at milling time t, the water vapor pressure $p_{H_2O}(T, t)$, Ar partial pressure $p_{Ar}(T, t)$, and equation of state for an ideal gas were used to quantify the amount of H_2 in the vessel over the course of the reaction. Details of the calculations are described in Note S1 in the ESI.†

The following metal, metal oxide, and metal carbide powders were used as purchased: Al (012-19172, Wako; purity > 99.5%), Ti (200-05202, Wako; > 98%), Zn (269-00212, Wako; > 90%), Fe (090-04781, Wako; > 98%), Mn (130-06732, Wako; > 98%), Sn (202-01502, Wako; > 95%), W (35613-42, nacalai tesque; > 99.9%), TiO_2-anatase (40167-21, Kanto Chemical Co. Inc.; > 98.5%), TiO (77126, Alfa Aesar; > 99.5%), Ti_2O_3 (205-18942, Wako; > 90%), WO_3 (205-10262, Wako; > 99.5%), SiO_2 (342890, Sigma-Aldrich; 99.5%), Fe_2O_3 (19518-15, nacalai tesque; > 95%), ZnO (ZNO06PB, Kojundo chemical laboratory Co. LTD.; > 99.9%), and WC (WWI01PB, Kojundo chemical laboratory Co. LTD; > 99%). Distilled water was used as produced by a commercial water distillation instrument (RFD240NC, Advantec). Seawater was collected at a beach in Hiroshima prefecture in Japan and used after filtration with a filter paper.

Safety protocol

The above-described experimental methods for the production of H_2 *via* mechanochemical reactions using a planetary ball mill were verified to be safe. It should be emphasized that monitoring the pressure in the vessel was a very important aspect of this study. This is because the combination of high revolution velocity (*ca.* >500 rpm) and long milling time (>1 h) may produce large amounts of H_2, *i.e.*, the pressure of the H_2 generated might be sufficiently high to break the vessel seal. Thus, in experiments such as this, it is critical to start H_2 production under very mild conditions. Specifically, the combination of a low revolution velocity (100 rpm) and short milling time (10 min) is

essential when a new metal and/or metal oxide is reacted with water. Under these mild conditions, the amount of H_2 produced by the mechanochemical metal–water reactions in the planetary ball mill will be small, and hence there will be no need for concern about the possibility of a significant increase in pressure inside the vessel. In fact, we started all our experiments under these safe conditions, and, to date, no accidents have occurred in our laboratory during ball-milling experiments. However, monitoring the internal pressure and temperature of the vessel during the mechanochemical reaction is recommended when a batch-type vessel is used to produce H_2.

Characterization

The chemical species in the generated gas were analyzed using gas chromatography (GC; SHIMADZU GC-2014) (Note S2, ESI†). Briefly, the gas generated in the vessel was collected in a sampling bag and injected into the GC instrument using a microsyringe. For qualitative analysis, the gas was evaluated by measuring the retention times and comparing the obtained values with those of standard gases such as H_2, O_2, N_2, CH_4, CO_2, and CO. For quantitative analysis, the amount of gas was estimated using a calibration curve for the signal area and gas concentration. The details of the GC measurements are presented in Note S2 in the ESI.†

Raman spectroscopy, X-ray diffraction (XRD), Fourier-transform infrared spectroscopy (FTIR), X-ray photoelectron spectroscopy (XPS) and scanning electron microscopy (SEM) measurements of the solid products were acquired using a spectromicroscope (LabRAM HR 800, HORIBA JobinYvon), X-ray diffractometer with Cu K_α radiation (SmartLab SE, Rigaku), spectrometer (FT/IR-4200, JASCO Corporation), and XPS spectrometer (KRATOS ULTRA2, Shimadzu), SEM instrument (N-3400, Hitachi), respectively. Samples of the products were collected from the solution in the vessel by filtration and/or centrifugation and then dried at 35 °C in a vacuum drier for 24 h prior to the measurements. In addition, after the mechanochemical reactions, samples of the reaction solution were analyzed by titration and using inductively coupled plasma optical emission spectroscopy (ICP-OES). The details of the characterization methods are described in Notes S4, S7–S9, S11, and S14 in the ESI.†

Results and discussion

Metal–water reactions triggered by mechanochemical milling

To mechanochemically react the metal with water, distilled water, metal powder, and tungsten carbide (WC) milling balls were placed in an Ar-purged WC planetary ball mill vessel (Fig. 1A) within a commercially available planetary ball-milling apparatus.[22,23,30–34] Six metal reactants—four typically used in studies on conventional metal–steam reactions (Al, Zn, Fe, and Mn) as well as Ti and Sn—were selected for this study. The metals were mechanochemically reacted with the distilled water, and the results of the *in situ* monitoring of the temperature T and pressure p of the gas in the vessel during milling are shown in Fig. 1B and C; T and p were found to be 30–38 °C and 2–8 bar, respectively, during milling. A high p of 8 bar, observed only for the Ti–water reaction, occurred principally because of the large amount of H_2 generated by this reaction: the 8 bar gas mixture was found to be composed of H_2 (87%), Ar (12%), and water vapor (<0.9%), as shown in Fig. S1 in the ESI.†

A chromatogram of the gas produced by the mechanochemical Ti–water reaction is shown in Fig. 1D. Strong H_2 and weak N_2 and O_2 signals, with an N_2/O_2 intensity ratio the same as that of air (see inset), were observed; no other gases were observed in significant quantities (Fig. S2, S3, Tables S1 and S2, ESI†). Thus, the mechanochemical reaction between Ti and water can be classified as an O_2-separation-free and zero-CO_2-emission method for producing high-purity (>99%) H_2.

The amounts of H_2 produced by the various systems as a function of milling time are shown in Fig. 1E. By 600 min, all the mechanochemical metal–water reactions had produced H_2 at levels of 0.15–6.9 mol mol_{metal}^{-1} (Table S3, ESI†). The metal–water reactions can be expressed as $xM + yH_2O \rightarrow M_xO_y + yH_2$ and $xM + 2yH_2O \rightarrow xM(OH)_{2y/x} + yH_2$, where M is the metal and x and y are the stoichiometric ratios for complete oxidation of the metal and complete reduction of the water, respectively. A H_2 yield of 100% corresponds to the situation in which all of the metal placed in the vessel is fully oxidized and consumed to produce H_2 (Table 1). Specifically, when the 2 mmol of metal reactant added to the vessel was fully oxidized by the reaction with an excess of water (560 mmol), and all the metal powder was consumed to produce H_2 (*i.e.*, there was no reduction of the oxidized metal), the H_2 yield (*e.g.*, 4 mmol for the reaction of Ti or 2 mmol for that of Zn) was defined as 100%. Moreover, it should be noted that oxygen was not released, but was instead trapped in the form of metal oxides (Table 1). [Note that here all the reactions are considered to be simple stoichiometric reactions, and the possibility of any catalytic activity or regeneration of the oxidized metal is neglected; for the reaction involving Ti, the possibility of catalytic activity and regeneration is discussed later (*vide infra*).]

With the exception of the Sn and Ti systems, the H_2 yields were 70–100% (Fig. 1F and G). Almost all the mechanochemical metal–water systems, therefore, produced H_2 efficiently at temperatures close to room temperature (30–38 °C). Note that under standard-state conditions [*i.e.*, 25 °C and 10^5 Pa (1 atm)], none of these hydrogen-producing metal–water reactions proceed because the passivation layer on the metal surfaces significantly hinders the reaction with water. The high efficiencies at low temperature are attributable to (i) mechanical passivation-layer destruction during milling, (ii) increased numbers of reactive sites because of the increased surface area generated by milling, (iii) the high exergonicity of H_2-producing metal–water reactions (Table S4, ESI†), and (iv) localized regions of high T and p generated by the impact of the milling balls (*vide infra*). In contrast, particular time profiles for the inefficient Al and Zn reactions were observed (Fig. 1E and F), which were attributed to an induction period, as discussed in Note S3 in the ESI.† In this report, we focus on the extraordinary amounts of H_2 produced by the mechanochemical reaction between Ti and

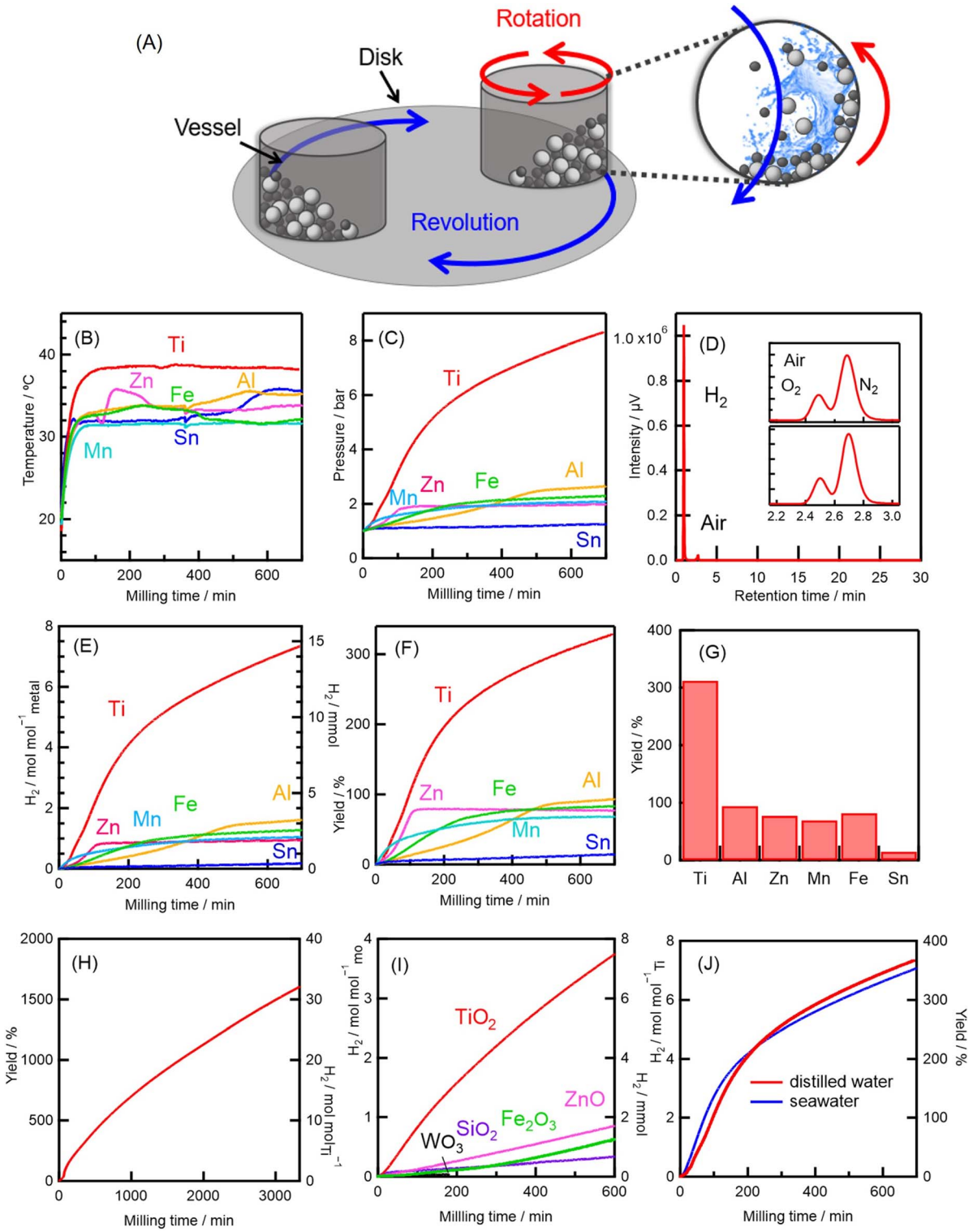

Fig. 1 Mechanochemical H_2-production reactions. (A) Schematic of mechanochemical metal–water reactions in a planetary ball mill vessel containing milling balls, water, and metal powder. (B–J) Experimental results for mechanochemical metal–water reactions triggered by milling with a WC medium at a revolution velocity of 400 rpm: (B) temperature and (C) pressure of the gas in the vessel measured *in situ* during milling. (D) Gas chromatogram of the gas generated by the mechanochemical Ti–water reaction. The upper and lower insets are chromatograms of air and an expanded view of the chromatogram in the main panel showing air contamination in the vessel, respectively. (E) Amount of H_2 produced, calculated from pressure and temperature measurements, *vs.* milling time. The left axis shows the H_2 amount normalized to the molar amount of the metal used in the reaction, and the right axis shows the H_2 amount produced using 2 mmol of metal. (F) H_2 yields *vs.* milling time. (G) H_2 yields after 600 min of milling various metals. (H) Yield (left axis) and amount (right axis) of H_2 produced by the mechanochemical Ti–water reaction over a longer period of milling using 0.5 mmol of Ti. (I) H_2 produced during mechanochemical reactions between metal oxides (mo) and water. (J) H_2 produced during mechanochemical reactions between Ti and distilled water or seawater.

Table 1 Metal–water reactions and H_2 amounts produced[a]

Metal	Chemical equation	H_2 produced at 100% yield (mmol) from 2.0 mmol of metal reactant
Al	$Al + 3H_2O \rightarrow Al(OH)_3 + 3/2H_2$	3.0
Ti	$Ti + 2H_2O \rightarrow TiO_2 + 2H_2$	4.0
Zn	$Zn + H_2O \rightarrow ZnO + H_2$	2.0
Fe	$Fe + 4/3H_2O \rightarrow 1/3Fe_3O_4 + 4/3H_2$	2.7
Mn	$Mn + 4/3H_2O \rightarrow 1/3Mn_3O_4 + 4/3H_2$	2.7
Sn	$Sn + H_2O \rightarrow SnO + H_2$	2.0

[a] Chemical equations for various metal–water reactions are given, alongside the H_2 amounts produced by complete oxidation of 2 mmol of the metal in the presence of an excess of water.

water. The details of each of the other reactions in Table 1 are discussed in Note S4 in the ESI.†

Extraordinary amounts of H_2 produced

The H_2 yield of the Ti–water reaction was 300% at 600 min (Fig. 1F and G); however, the reaction was not complete at this time, and the final yield was 1600% (Fig. 1H). Thus, H_2 was continuously produced until all the water in the vessel had been consumed. Note that the yield was determined with respect to the amount of the metal reagent because an excess of water was placed in the vessel to allow quasi-continuous H_2 production. Compared to the Ti–water reaction, the reaction between water and the WC milling medium in the absence of Ti produced relatively little H_2 (<7%) (Fig. S6, Note S5, ESI†). In addition, we repeated our experiment to verify that the mechanochemical Ti–water reactions produced an extraordinary amount of H_2, and the reproducibility of this result was confirmed. Specifically, the different repetitions produced H_2 reaction yields that were within 10% of each other (Fig. S7, Note S6, ESI†).

To explore this extraordinary H_2 production, we mechanochemically reacted various metal oxides—TiO_2, ZnO, Fe_2O_3, WO_3, and SiO_2—with distilled water (Fig. 1I). All these reactions, with the exception of that involving TiO_2, produced small amounts of H_2, similar to the amount produced by the reaction between the milling medium itself and water (Fig. S6, Note S5, ESI†). In addition, as mentioned above, the H_2 yields of the reactions of each of the unoxidized metals (except Ti) were <100% (Fig. 1G). Furthermore, since oxide reduction reactions are highly endothermic (250–1300 kJ mol^{-1}, see Table S5, ESI†), they cannot proceed under mild conditions at close to room temperature (RT = 2.5 kJ mol^{-1} at $T = 300$ K). Thus, it does not seem appropriate to categorize the reactions with metals and/or oxides, with the exception of those with Ti and its oxide, as catalytic H_2-production reactions. However, the mechanochemical TiO_2–water reaction produced a significant amount of H_2—nearly half that produced by the Ti–water reaction (Fig. 1E and I). An analysis based on gas chromatography (GC) indicated that the amounts of other gases in the gas mixture generated by the TiO_2–water reaction (<1%) were negligible (Fig. S8, Note S7, ESI†). Therefore, TiO_2 must have been responsible for the extraordinarily large amounts of H_2 yielded by the Ti–water reaction.

The fact that a similar, extraordinarily large quantity of H_2 was produced when seawater, rather than distilled water, was used is noteworthy (Fig. 1J). In addition, it was verified that Cl^- remained in the solution in the vessel, and Cl_2 gas was not produced by the mechanochemical Ti–seawater reaction (Fig. S9, Note S8, ESI†). Although low-grade water is not usually used to produce H_2 *via* methods such as water electrolysis, our method facilitates the use of low-grade water such as seawater as a H_2 feedstock. The difference between the H_2-production behavior of the Ti–distilled water and Ti–seawater reactions was minimal. In fact, different H_2-production behavior is observed when aqueous solutions containing different salts are reacted with metals, and this variation can be explained in terms of the properties of the salts (Note S8, ESI†).

In addition, it should be emphasized that Ti typically does not react, even with hot water, and is sufficiently inert for use in human orthopedic and dental implant applications. However, in our experiments, Ti was very reactive when subjected to mechanochemical milling in water, producing large amounts of H_2. This behavior was attributed to a specific property of metallic Ti: it has a high oxygen affinity at high temperatures,[35] which facilitates efficient H_2 production from water. Furthermore, we found evidence that the collisions between milling balls produced localized high temperatures and pressures in the milling vessel (*vide infra*).

Mechanocatalytic H_2 production and mechano-cocatalytic activity of the milling medium

We investigated the use of different milling media for mechanochemical metal–water reactions to gain insights into the mechanisms underlying the extraordinary ability of Ti and TiO_2 to produce H_2. The amounts of H_2 produced using the WC, stainless steel (SUS), and ZrO_2 milling media (vessel and balls) were compared (Fig. 2A). Extraordinarily high-yield H_2 production was observed with either a WC or SUS milling medium at 400 rpm. In contrast, when the milling medium was ZrO_2, a H_2 yield of 100% was obtained at the same milling speed, and even at 700 rpm, extraordinarily high yields of H_2 were not observed (Fig. 2A).

To investigate the effect of the milling medium on the H_2 production yield, we conducted several analyses. First, as the use of light milling balls can reduce the mechanical energy and reaction efficiency of a system, even at a high revolution velocity, we calculated the collision energies in the systems containing the three different milling media using eqn (S25)–(S28) (Note S12, ESI†) and the values in Table S7 (ESI†). Although ZrO_2 has the lowest density among the media, at 700 rpm the cumulative collision energy of the ZrO_2 milling medium was significantly higher that those for the other two systems at 400 rpm (the ratio between these collision energies for the different media was $ZrO_2 : WC : SUS = 4.8 : 2.0 : 1.0$). Despite its high collision energy, the system with the ZrO_2 milling medium was not able to produce extraordinary quantities of H_2. Moreover, we verified that extraordinary quantities of H_2 were produced (~150% yields) when Ti and WC powders were milled together in a ZrO_2 vessel with ZrO_2 milling balls

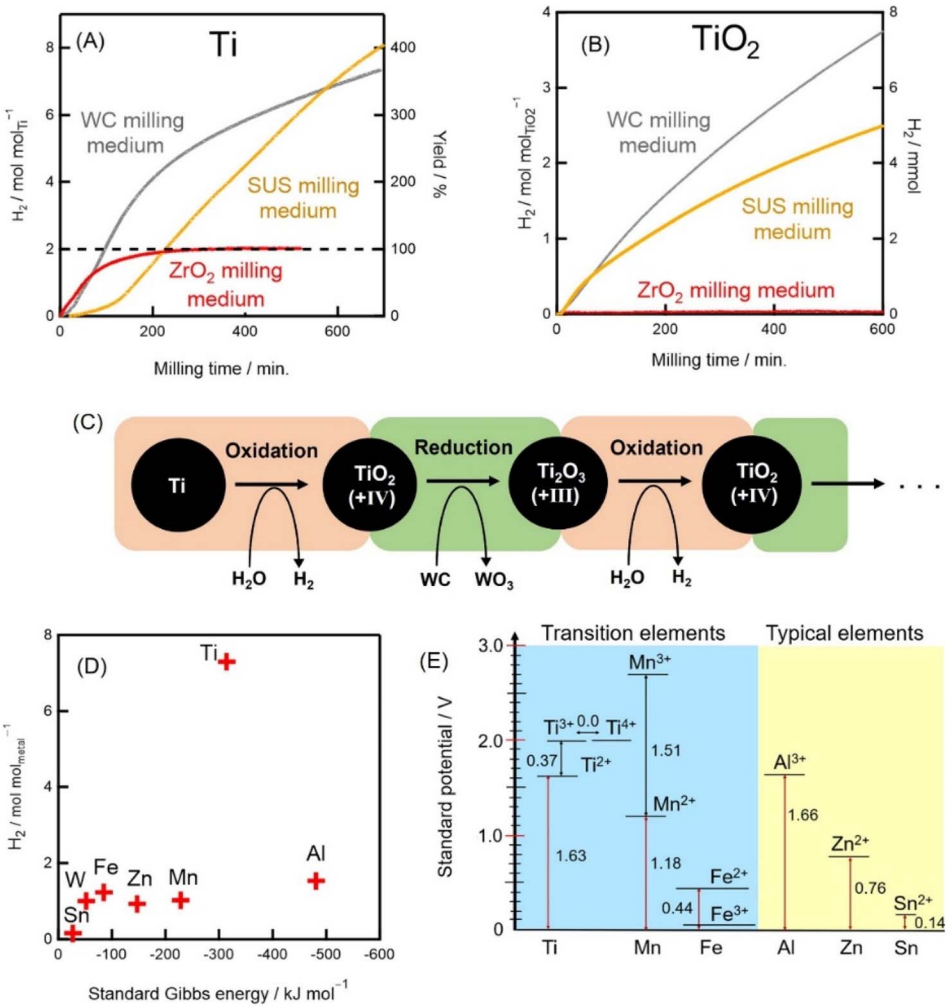

Fig. 2 Regeneration of titanium oxide catalyst by non-oxide milling-medium mechano-cocatalyst. Dependence of H_2 production on the milling medium (vessel and balls) during the mechanochemical reactions of (A) Ti and water and (B) TiO_2 and water. The gray, yellow, and red curves indicate results obtained using WC, stainless steel (SUS), and ZrO_2 milling media, respectively. The H_2 amounts and yields are shown on the left and right axes, respectively. The revolution velocities of mechanochemical reactions of (A) using WC, SUS, and ZrO_2 milling media were set to 400, 400, and 600 rpm, respectively, and those of (B) were set to 400 rpm. (C) Schematic of H_2 production *via* mechanochemical Ti/titanium oxide–water reactions. For clarity, a cyclic reaction involving TiO_2 and Ti_2O_3 is displayed; TiO_2, TiO, and Ti_2O_3 produce similar amounts of H_2 (Fig. 3). (D) H_2 amount produced by various mechanochemical metal–water reactions *vs.* standard Gibbs energy. (E) Standard potentials of various transition metal and typical metal cations.

(Fig. S13†). In conclusion, the presence of WC and/or SUS must in some way be essential to the production of extraordinary quantities of H_2 by mechanochemical Ti/TiO_2–water reactions.

Second, continuing our exploration of the role of the milling medium, we considered its composition. Significantly higher H_2 yields were realized when a milling medium devoid of metal oxides was used. This experimental evidence suggests that TiO_2 is mechanochemically reduced by WC and SUS, and that the product of the TiO_2 reduction reaction is used to produce extra H_2. As further experimental evidence, the reaction between TiO_2 and water produced significant amounts of H_2 when the milling medium was WC or SUS (Fig. 2B). In contrast, when ZrO_2 was used as the milling medium for this reaction, H_2 was not generated. ZrO_2, as a fully oxidized material (the electron configuration of Zr^{4+} is [Kr]$4d^0 5s^0$), has no valence electrons, and these are required for the reduction of TiO_2 (Ti^{4+}: [Ar]$3d^0 4s^0$). Thus, the ZrO_2 milling medium did not regenerate the TiO_2 catalyst and H_2 was not produced (Fig. 2B). However, W^{4+} ([Xe]$4f^{14}3d^2 4s^0$) in the WC milling medium and Fe ([Kr]$3d^6 4s^2$), Cr ([Kr]$3d^5 4s^1$), and Ni ([Kr]$3d^8 4s^2$) in the SUS milling medium have multiple valence electrons that can be used to reduce TiO_2. In other words, an oxygen acceptor is required to produce H_2, and there were no oxygen acceptors in the fully oxidized system containing TiO_2, water, and the ZrO_2 milling medium; hence, no H_2 production was observed for this system.

Third, we measured the XRD patterns of the solid products of the mechanochemical TiO_2–water reactions. Peaks assignable to TiO and Ti_2O_3 were observed in the patterns of the reaction product mixtures generated using the WC and SUS milling media (Fig. S14 and S15, ESI†). Moreover, for the reduction of TiO_2 by WC or SUS, the standard Gibbs energies ($\Delta_r G^\circ$) are in the range of −9 to 400 kJ mol^{-1}, significantly lower

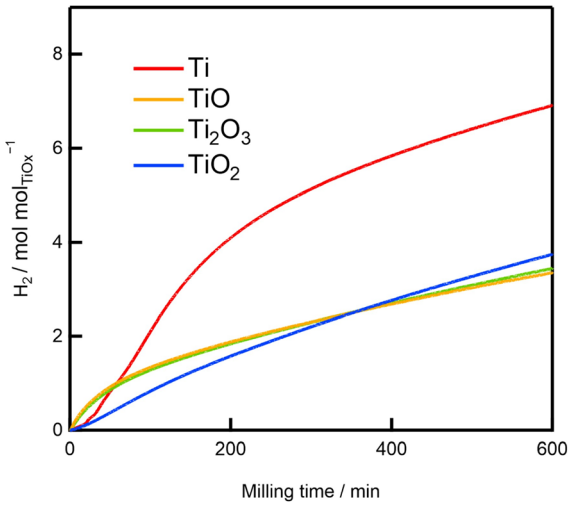

Fig. 3 Amount of H_2 produced as a function of milling time during the mechanochemical reactions between water and Ti or various titanium oxides. The milling medium was WC and the revolution velocity was 400 rpm.

than $\Delta_r G°$ for the reaction of TiO_2 generating O_2 gas (884 kJ mol^{-1}) (Tables S5 and S8, Note S15, ESI†). Therefore, considering the collision energies, valence electron configurations of the transition metals in the milling medium, XRD data, and thermodynamic states of the systems, we conclude that H_2 was produced from water *via* catalytic mechanochemical processes in our experiments.

In general, H_2 evolution ceases when the catalyst for the H_2-production reaction has been inactivated and is not regenerated. However, in the present system, Ti reacted continuously with water to produce H_2 (Fig. 1E–J). Furthermore, when titanium oxides (TiO_2, Ti_2O_3, and TiO) were subjected to the same ball-milling treatment as Ti, they also acted as catalysts, continuously producing large amounts of H_2 (Fig. 3). This was because the catalyst (Ti and/or titanium oxides) was regenerated by the milling medium (balls and vessel). In other words, the milling medium (WC or SUS) can be described as a cocatalyst or sacrificial reductant as it regenerates the Ti and/or titanium oxide catalyst, facilitating continuous hydrogen production (Fig. 2B and C). This finding, that a mechano-cocatalyst can regenerate a catalyst, is a novel concept in mechanochemistry.

Another piece of evidence supporting our conclusion that Ti and titanium oxide mechanocatalysis was responsible for the extraordinary H_2 production is the fact that the H_2 production *versus* time profile of the mechanochemical Ti–water reaction includes a turning point: H_2 production slowed at 200 min (Fig. 1E). However, such a turning point was not observed for the mechanochemical TiO_2–water reaction (Fig. 3). Hence, H_2 was produced by the mechanochemical Ti–water reaction *via* a two-step process, with the dominant H_2-production process changing from the Ti–water reaction to the titanium oxide–water reaction at the turning point; this is also supported by the fact that it is clear from the slopes shown in Fig. 3 that the rate of the second stage of the Ti–water reaction is the same as the rate of the TiO_2–water reaction. In addition, the reactions of TiO and Ti_2O_3 exhibited similar turning points, albeit at earlier times during the reactions (~30 min). This is because TiO (+II) and Ti_2O_3 (+III) have higher oxidation numbers than metallic Ti (0), and hence they were more rapidly converted into TiO_2 (+IV).

Mechanocatalysis is a recent focus area in research on mechanochemistry; for example, mechanocatalysts for the cross-coupling syntheses of organic molecules or polymers can be supplied by the abrasion of milling balls during solid-phase (dry) milling.[21,23,36] In contrast, in the present H_2-production reaction, the mechanocatalyst is the metal/metal oxide placed in the vessel, and the mechano-cocatalyst is produced by abrasion of the milling medium during wet milling. The reaction between TiO_2/Ti and water in the presence of the WC mechano-cocatalyst resulted in extremely high-volume, continuous H_2 production, and the presence of the cocatalytic byproduct (WO_3) was verified using FTIR (Fig. S10, ESI†), Raman (Fig. S11, ESI†), and X-ray photoelectron (Fig. S12, ESI†) spectroscopies.

Furthermore, it should be emphasized that continuous H_2 production *via* Ti mechanocatalysis was also realized using the SUS milling medium (Fig. 2A and B). In this system, the Fe content of the SUS milling medium acted as a mechano-cocatalyst, facilitating the production of extraordinary quantities of H_2 *via* mechanochemical Ti/TiO_2–water reactions, and the presence of the cocatalytic byproduct (Fe_3O_4) in the vessel after the reaction was verified *via* XRD (Fig. S15, ESI†). In addition, note that SUS is much more widely used than WC. In fact, the SUS milling medium used in our study is commercially sold at a price 50 times lower than that at which the WC milling medium is sold. The cost-effectiveness of SUS is an additional advantage that should facilitate the utilization of this mechanocatalytic process as a practical H_2-production method.

Oxidation–reduction potentials and cyclic H_2 production

To thermodynamically explore the relationship between the amount of H_2 produced and the nature of the metal, we first evaluated the standard Gibbs energies ($\Delta G°$) using standard electrode potentials (oxidation–reduction potentials) (Table S3, Note S15, ESI†).[37] These potentials are essential parameters for characterizing hydrogen evolution *via* the electrocatalytic, photocatalytic, and chemical reactions of water. The amount of H_2 produced by the different metals is proportional to the magnitude of $\Delta G°$, in common with metal corrosion trends (electrochemical series). Although it is apparent that the magnitude of $\Delta G°$ for the oxidation of Ti is greater than $|\Delta G°|$ for the oxidation of most of the other metals (Fig. 2D), strikingly, the amount of H_2 produced using Ti significantly deviated from the abovementioned trend of proportionality with $\Delta G°$.

Next, we compared the standard potentials of metals that exist as cations in different oxidation states (Fig. 2E).[37] This analysis is very important because the metals used in the present study are transition elements that can exist in various oxidation states, and hence there are several oxidation–reduction potentials for each transition-metal atom. Note that the three Ti cations (Ti^{4+}, Ti^{3+}, and Ti^{2+}) have similar redox potentials (the potential differences are within 0.37 V), as shown in Fig. 2E. In our experiments, significant amounts of H_2 were

produced using TiO and Ti_2O_3—approximately equal to that produced using TiO_2 or half that produced using Ti (Fig. 3). Thus, in the presence of the milling-medium mechanococatalyst, titanium oxides containing Ti in various oxidation states produced large amounts of H_2 owing to the regeneration of the catalyst, which occurred because of the similarity between the redox potentials of the three Ti cations.

The H_2 produced by a cyclic Ti-species system was examined in a pioneering study of a solar thermochemical reaction;[38] a reversible TiO_2/TiO_x ($x < 2$) cycle involving Zn produced H_2 continuously at a high temperature (~2500 K). In contrast, in the present study, continuous H_2 production was achieved *via* a reversible TiO_2/Ti cycle at temperatures close to room temperature (30–38 °C), and hence our system represents a new approach for room-temperature thermochemical water splitting. However, it should be noted that the mildness of the conditions under which this mechanochemical reaction apparently proceeds belies the fact that highly reactive sites exist between the colliding balls (*vide infra*). Titanium hydroxide is another potential byproduct of the room-temperature H_2 evolution reaction, but the formation of this mineral during the reaction between Ti and water has not been reported. In general, when metallic Ti reacts

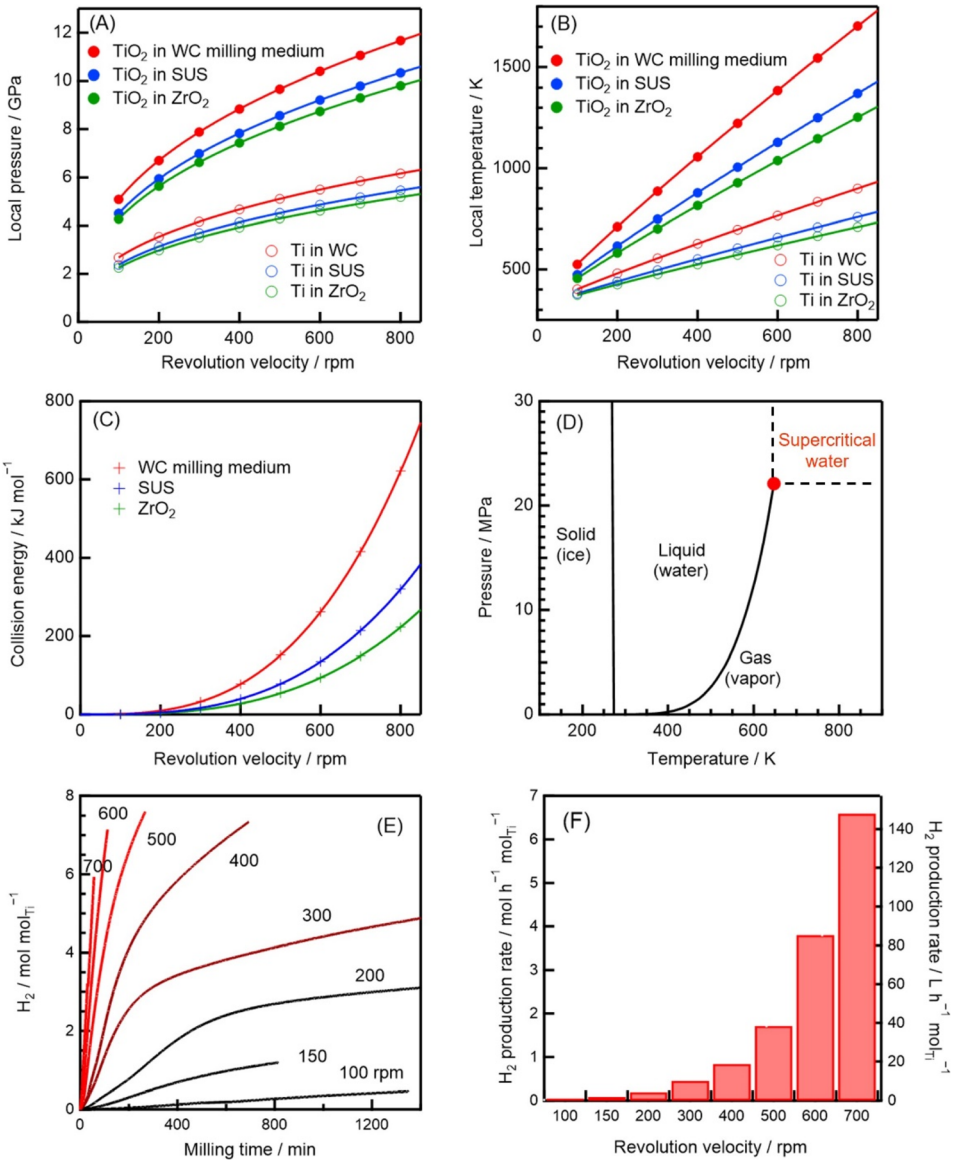

Fig. 4 Calculated collision-impact and experimental H_2-production rate data. Calculated (A) local impulsive pressure, (B) local impulsive temperature, and (C) cumulative collision energy for a 10 s period *vs.* revolution velocity for the different reaction systems. The red, blue, and green curves represent the data calculated for the WC, stainless steel (SUS), and ZrO_2 milling media, respectively. Solid and open circles represent the data calculated for the TiO_2 and Ti powders, respectively. (D) Pressure–temperature phase diagram of water. The red solid circle highlights the vapor–liquid critical point; beyond this point, supercritical water exists. (E) Experimental time profiles for H_2 production by milling Ti in water at various revolution velocities. (F) H_2-production rates obtained from the initial slopes in panel E. The left and right axes show the H_2-production rates in molar (mol h^{-1} mol_{Ti}^{-1}) and standard-state volume (L h^{-1} mol_{Ti}^{-1}) units, respectively.

with water at high temperatures (*i.e.*, during a hydrothermal reaction), the principal product is TiO_2 (rutile), although Ti_2O_3 and TiO products have also been reported.[39] These literature results are in line with our observations in this study.

In a similar well-known cyclic system, CeO_2 functions as a catalyst regeneration material.[40] This catalyst regeneration process, which operates owing to the ease of Ce^{3+}/Ce^{4+} interconversion, has been used to produce H_2 by means of thermochemical water splitting[10,16] and in commercial catalytic convertors in vehicles. The titanium–oxygen phase diagram indicates that TiO_2 is highly reducible at high temperatures.[41] In particular, the (110) surface of TiO_2 is easily reduced to produce oxygen vacancies[40] and has been characterized as being similar to the reducible CeO_2(111) surface.[40]

Collision impact and thermodynamic states in the regions between striking balls

To investigate the TiO_2 reduction (catalyst regeneration) reaction, we computed the local p and local T in the region of contact between two balls (~50 μm) during impact ($\sim 10^{-6}$ s), as well as the collision energy, based on Hertz theory (Note S12, ESI†).[42,43] This theory has been demonstrated to predict values for the instantaneous p and T in a planetary ball mill in reasonable agreement with experimental values, verifying that solid-material phase transitions occur during mechanical ball milling.[22–25,30,32,44,45] We show the instantaneous p values of Ti between colliding balls when WC, SUS, and ZrO_2 are used as the milling media in Fig. 4A. Values of p of 3–6 GPa ($3–6 \times 10^4$ bar) were computed for revolution velocities of 200–700 rpm. Differences of 14–20% among the calculated p values for the milling media were obtained, and p was calculated as 6–11 GPa for TiO_2. The difference between the calculated p values for Ti and TiO_2 is ascribable to the different mechanical properties of these media, including their different Young's moduli and Poisson's ratios (Tables S6 and S7, Note S15, ESI†).

We calculated the local T between striking balls (Fig. 4B) based on the fact that the instantaneous p generates an increase in T, dependent on the thermal properties and tribology of the milling material, during collisions (Note S12, ESI†). The local T was obtained by summing the measured bulk T (20–38 °C) and calculated instantaneous ΔT. For the WC balls, the local T values were 600 and 1000 K for the Ti and TiO_2 systems, respectively, when the revolution velocity was 400 rpm, and 500–800 and 700–1600 K, respectively, when the revolution velocity was 200–700 rpm (Fig. 4B). High p (~GPa) and T (~1000 K) have been experimentally observed in the regions between striking balls in milled samples; for example, instances of high T and p were observed during Al_2O_3 (ref. 24 and 44) and TiO_2 (ref. 22, 25 and 45) phase transitions.

By summing the kinetic energies of the individual balls, the collision energy was determined (Note S12, ESI†). For instance, a plot of the cumulative collision energy for 10 s *versus* the revolution velocity (Fig. 4C) indicates that 100–800 kJ mol^{-1} of energy was continuously released when the WC milling medium was used with a revolution velocity in the range of 400–900 rpm. Such energies are significantly higher than the activation energies of all the metal–water reactions, which are in the 8–50 kJ mol^{-1} range (Table S4, Note S15, ESI†); they are also considerably higher than the $\Delta_r G^\circ$ values for the reduction of TiO_2 by the milling medium (−9 to 380 kJ mol^{-1}, Table S8, Note S15, ESI†). Furthermore, collisions occurred continuously and the reaction proceeded continuously, up to a reaction time of 1200 min (Fig. 4E).

Thus, three key conclusions can be summarized by comparing the collision-impact and thermodynamic data. First, the local T (~1600 K) is of the same order of magnitude as the temperature required for continuous H_2 production based on a solar thermochemical reaction with a reversible TiO_2/TiO_x cycle (~2500 K).[38] Second, high temperatures reduce the Gibbs energy such that the mechanocatalytic reduction of titanium oxide becomes exergonic (Table S8, Note S15, ESI†). Third, TiO_2 is reduced when it is mechanochemically milled at low temperatures.[22,46] To summarize, in the present reaction system, continuous H_2 production *via* TiO_2 reduction occurs thanks to the negligible differences between the standard potentials of the various Ti cations, the reducibility of the TiO_2 surface, high collision energies, and the lowering of $\Delta_r G$ in the localized regions of high p and T.

Supercritical water and H_2-production rate

In addition, the calculated local p and T values (11 GPa and 1600 K) were significantly higher than the water liquid–vapor critical pressure (p_c = 22.1 MPa) and temperature (T_c = 647 K), respectively (Fig. 4D).[37] Hence, chemical reactions occurring near the colliding balls were exposed to supercritical water, which is a highly reactive oxidant.[47,48] In other words, H_2 was efficiently released during water reduction because supercritical water is a powerful oxidizing agent. Indeed, it is known that supercritical water significantly increases the H_2-production rates of reactions involving metals,[49] organic molecules,[50] and biomass.[13] Higher milling velocities resulted in increased H_2-production rates (Fig. 4E). In fact, the initial slopes in Fig. 4E indicate that the H_2-production rate was 300 times greater for milling at 700 rpm (corresponding to a local T of ~1550 K) than for milling at 100 rpm (corresponding to a local T of ~500 K), and significantly enhanced H_2-production rates are known to occur when the thermodynamic state lies above the critical temperature (647 K). In particular, using WC milling media, a revolution velocity of >500 rpm generated supercritical water (the local T and p were 700 K and 5 GPa, respectively; Fig. 4A and B). Supercritical water was easily accessed owing to the high revolution velocities and/or the use of TiO_2, which has a high Young's modulus and low thermal conductivity (Fig. 4A and B; Table S6, ESI†).

To experimentally disentangle the effect of the locally high T from other influences, we analyzed the products of the mechanochemical reactions between water and the other metals (*i.e.*, Al, Zn, Fe, Mn, and Sn) using X-ray diffraction (XRD) (Fig. S4, ESI†). We were motivated to perform these measurements, because metal–steam reactions have different products (hydroxides and other metal oxides with different oxidation numbers) depending on the reaction temperature (Note S4, ESI†). Our detailed XRD analyses in fact indicated that all the products of the different

metal–water reactions were generated at high temperatures (600–1900 K). These experimental results for the mechanochemical reactions between water and five different metals are consistent with the reactions proceeding in localized regions of high temperature, in line with our theoretical analysis.

Furthermore, it is well-known that during mechanochemical ball milling, localized regions of high p and T are generated.[22–25,44,45] When milled in a planetary ball mill, anatase TiO_2 is converted into a high-pressure phase of TiO_2 (TiO_2-II, also known as α-PbO_2-type, columbite, or srilankite TiO_2),[22,25,45] and this phase transformation is known to occur at pressures of >1 GPa, as shown in the p–T phase diagram of this material.[51] Interestingly, naturally occurring α-PbO_2-type TiO_2 has been found in a meteorite impact crater on the earth.[26] Moreover, milling γ-Al_2O_3 in a planetary ball mill can also result in a phase transformation, with α-Al_2O_3 being generated in the T range of 1000–1500 K owing to the mechanical energy imparted to the system by milling.[24,44] Furthermore, mechanical energy has also been used to transform γ-AlOOH, using a vibration mill, into α-AlOOH at 800–873 K; in this case, the increase in surface area also played a role.[24] All of the abovementioned mechanical milling studies[22–25,30,32,44,45] were conducted at room temperature without thermal heating. Therefore, the use of a mechanical ball mill, and a planetary ball mill in particular, allows easy access to high T and p in the vessel. Another important point is that the surface area of the powdered materials increased during ball milling, which has been known to cause phase transitions owing to the modulation of ΔG for the polymorphs.[52,53] This effect has been observed during relatively low-energy ball milling for metal oxides[24] and molecular crystals[54] (milling in a vibration ball mill at frequencies of 20–30 Hz).[24,54] However, it is important to remember that in the present study efficient H_2 production occurred at high revolution velocity (>400 rpm) using the planetary ball mill, thanks to localized high T and p conditions.

Finally, we evaluated the H_2-production rate as a function of the revolution velocity (Fig. 4F). The H_2-production rate was 150 L h^{-1} mol_{Ti}^{-1} at 700 rpm (when the power consumption was 0.26 kW), which corresponds to an energy-consumption-normalized H_2-production rate of 0.58 m^3 kW h^{-1} mol_{Ti}^{-1}. Compared to a typical H_2-production rate for alkaline water electrolysis [42 m^3 h^{-1} at 70 °C and 200 kW, corresponding to 0.21 m^3 kW h^{-1} (ref. 4)], the H_2-production rate obtained in this study is high, although a direct comparison is somewhat difficult as the units are different. However, we normalized all our production rates to the consumed power, and over the range of revolution velocities investigated, 700 rpm was found to be the highest-efficiency condition, *i.e.*, the condition at which the amount of H_2 produced per unit of energy consumed was maximized (Note S13, Fig. S16, ESI†). Thus, we calculated the energy consumption with respect to the H_2 produced at 700 rpm and compared the result with the corresponding value for H_2 production *via* alkaline electrolysis. Energy consumption values of 1.72 kW h m^{-3} mol_{Ti}^{-1} and 4.76 kW h m^{-3} were obtained for the mechanochemical process in this study and alkaline electrolysis, respectively, as reciprocals of the abovementioned energy-consumption-normalized H_2-production rates.

Comparison with previous studies

The production of H_2 from water *via* the transformation of mechanical energy into chemical energy has been reported by a few groups.[27–29] Mechanochemistry allows H_2 to be generated under very mild conditions. Magnetically stirring various metal oxides (*e.g.*, NiO) in a glass beaker containing water produces small amounts of H_2 (maximum production rate: 0.035 mol h^{-1} mol_{NiO}^{-1}) and O_2, and conversion efficiencies of up to 4.3% have been reported.[27] This reaction occurs *via* a mechanism involving water and the metal oxide, driven by the mechanical force exerted by the stirrer bar on the glass beaker. However, the authors of this study reported no H_2 evolution using TiO_2, and they stated that TiO_2 was mechanochemically inert for the generation of H_2.[27] In other papers, written by different research groups, two H_2-production systems based on ball milling were reported, and these can both be classed as O_2-free methods. H_2 generation from water was triggered by milling quartz powder using a vibration mill,[28] and the H_2-production rate was low, 0.0043 mol h^{-1} $mol_{SiO_2}^{-1}$, which is more than 250 times lower than the value obtained in the present study (1.2 mol h^{-1} mol_{Ti}^{-1}, the rate at 3 h; Fig. 1E). In the other system using a planetary ball mill reported in the literature, the friction between the SUS milling balls and vessel produced H_2 from water in the absence of a metal reactant, but the amount of H_2 generated was small at a revolution velocity of 400 rpm.[29] In contrast, in the present study, although the same milling conditions were used (SUS milling medium, 400 rpm), the amount of H_2 generated without Ti was 35 times less than that generated with Ti [compare Fig. S6, ESI† (0.4 mmol) and Fig. 1E (14 mmol) at 600 min]. Therefore, H_2 production was significantly enhanced in the presence of Ti, and we can conclude that the mechanocatalytic Ti–water reaction (thermochemical cycle) is extremely advantageous as a method for efficient H_2 production based on ball milling.

In the present study, the highest amount of H_2 ever produced by means of ball milling (6.6 mol h^{-1} mol_{Ti}^{-1}, Fig. 4F) was recorded. The mechanochemical Ti/titanium oxide–water reaction continuously produced H_2, and yields of >100% were achieved *via* cyclic mechanocatalysis. In addition, the mechanochemical reactions between water and TiO, Ti_2O_3, and TiO_2 all yielded large amounts of H_2 owing to the regeneration of the catalyst (Fig. 3). However, no H_2 was produced when TiO_2 and water were placed in a glass vessel and agitated using a magnetic stirrer bar.[27] Therefore, we conclude that high-energy ball milling altered the reaction itself, owing to the generation of impulsive increases in the local p and T between colliding balls, to 11 GPa and 1600 K, respectively. Indeed, in the present study at low revolution velocities (100–200 rpm) as well as in previous studies,[27–29] the mechanical energy imparted by milling was the dominant factor triggering H_2 generation. However, under conditions of high mechanical energy, using the planetary ball mill at high revolution velocities (>400 rpm), the dominant factor changes to the high local T generated by the milling process, and the mechanochemical Ti/titanium oxide–water reaction causes thermochemical water splitting, resulting in the extraordinary H_2

production. In addition, this extraordinary H_2 generation is further enhanced in the presence of supercritical water.

Indeed, easy access to supercritical water during high-energy mechanochemical milling has been shown to be invaluable to facilitate the production of H_2 using metals,[49] organic molecules,[50] and biomass[13] as reagents. In these demonstrations, a specific vessel was used to reach the high p (>22.1 MPa) and high T (>647 K) of supercritical water. However, the present method does not require such vessels, with access to supercritical water being realized simply by switching the planetary ball mill to a high revolution velocity. In particular, H_2 is efficiently released by the reduction of water because supercritical water is a powerful oxidizing agent,[47–49] promoting oxide formation and preventing the release of O_2 gas. Furthermore, as another important aspect, high-energy ball milling typically produces large numbers of defects in solid materials, and these can function as highly active reaction sites[22,55] for the generation of H_2.[16,40] Specifically, Ti^{3+}, Ti^{2+}, and oxygen vacancies are known to promote H_2 generation during TiO_2 photocatalysis and electrocatalysis.[7,22] In addition, it is important to remember that the dynamics of the surface are important factors in mechanochemistry. For example, the reduction and coarsening of particles and crystallites have significant roles in material transformations, especially during low-energy ball milling (*e.g.*, in a vibration mill at vibration frequencies of 20–30 Hz)[24,54] owing to the modulation of ΔG for different polymorphs.[52,53] In contrast, in the present study, we conducted milling experiments at high revolution velocities (>400 rpm) using a planetary ball mill.

When evaluating the motivation for the practical implementation of this H_2-production method, it should be noted that various thermochemical water-splitting systems that continuously produce H_2 *via* reversible metal–metal-oxide cycling at high temperatures (1000–2000 K), using very large facilities (such as a nuclear reactor or heliostat field of a solar tower power plant, corresponding to footprints > 20 m × 20 m), have been reported.[56,57] However, in this study, we demonstrated high-energy ball milling with water for continuous near-room-temperature H_2 production using a compact (50 cm × 40 cm × 30 cm) reactor. The use of such equipment proves that the development of small-scale thermochemical water-splitting instrumentation is feasible; rather than requiring a large facility, production can be realized on the laboratory scale. Hence, on-site and on-demand H_2 production, for use as required, is achievable. Although the adjective "high-energy" is used to describe the milling process, the power consumption in our study was, in fact, low: 1.5 A × 100 V = 0.15 kW at 400 rpm and 2.6 A × 100 V = 0.26 kW at 700 rpm. The use of low-power, compact equipment renders this reaction even more promising for on-site, on-demand H_2 production.

It is important to note that the release of H_2 gas during the reaction is required for safety. Indeed, the pressure inside the vessel was so high that a long reaction time (*e.g.*, >1 week) was not possible for safety reasons, and the instrument we used was designed with a safe-pressure limit of 10 bar. Thus, the future development of a reactor with H_2-gas flow and a water injection system is important for the implementation of truly continuous production, as well as for a complete evaluation of the energy efficiency of the method.

In addition, it should be mentioned that when all of the milling medium (WC or SUS) is oxidized, the catalyst (Ti and/or titanium oxides) may cease to be regenerated. In fact, when ZrO_2, which is a fully oxidized material, was used as the milling medium, it did not regenerate TiO_2, and hence no H_2 evolution was observed for the reaction of water with TiO_2 (Fig. 2B). Under such conditions, determining how long a milling medium can be used for catalyst regeneration is important. The WC milling vessel and milling balls used in our experiments had been in use for 10 years (mechanochemical reaction time ~5000 h) and 5 years (~2000 h), respectively, without replacement, prior to the experiments reported herein.

To further understand the mechanocatalytic process, investigating the oxidation states in the system should prove fruitful. For instance, X-ray absorption fine structure (XAFS) measurements, performed at a synchrotron facility, can be used to determine oxidation states, and such analysis as a function of reaction time could be a powerful tool. *In situ* XRD and Raman measurements, acquired during the mechanochemical reactions, could also be used to track the formation of the solid products in the milling vessel in real time.[58,59]

Conclusions

In summary, metals and metal oxides (Al, Ti, Zn, Fe, Mn, Sn, and their oxides) were mechanochemically milled in water using a planetary ball mill, and H_2 was produced with a purity of >99% in each case. High H_2 yields were obtained at temperatures close to room temperature (30–38 °C) using this method, which is also O_2-separation-free and does not generate CO_2. In particular, the mechanochemical Ti–water reaction continuously produced H_2 until the water in the vessel had been completely consumed. High-volume H_2 production—16-fold enhancement of the yield expected for complete reaction of the Ti reagent—was observed. This extraordinary level of H_2 production was attributed to a cyclic mechano-catalytic reaction involving water and TiO_2/Ti in which the non-oxide (WC or SUS) milling medium acted as a mechano-cocatalyst. The reaction process of this H_2 production corresponded to room-temperature thermochemical water splitting, which is a novel concept in the fields of mechanochemistry and thermochemical water splitting.

In this study, H_2 production occurred in localized volumes, in the thermodynamic region beyond the gas–liquid critical point of water (p > 11 GPa, T > 1600 K). The fact that the water was in a supercritical state meant that the rate of H_2 production was accelerated by a factor of 300; H_2 was efficiently released by water reduction by virtue of the fact that supercritical water is a powerful oxidizing agent. In addition, low-grade water (*e.g.*, sea, rain, and river water) is able to be used as the H_2 feedstock for the mechanochemical metal–water reaction. Furthermore, a compact reactor with low electrical power requirements can be used, which makes this reaction process suitable for on-site, on-demand H_2 production. This highly efficient, simple system emits no CO_2 and produces H_2 in a low-cost, environmentally

friendly manner. Although in this study a novel method for generating H_2 from water based on a new mechano-cocatalytic reaction mechanism was discovered, further optimization of the mechanochemical parameters or extension of the method to include other metals and/or metal oxides may afford improved reaction systems.

Data availability

The data supporting this article have been included as part of the ESI.†

Author contributions

T. Y., S. A., N. I., S. S., Y. M., T. M., and K. S. designed research. T. Y., S. A., N. I., S. S., Y. M., T. M., and K. S. performed research. T. Y., S. A., S. S., Y. M., T. M., and K. S. analyzed data. K. S. planned and supervised the research and wrote the paper with input from all the other authors.

Conflicts of interest

There are no conflicts to declare.

Acknowledgements

We acknowledge Y. Kimura and T. Takeda of Fritsch Japan Co., Ltd. for helpful discussions on mechanochemical instrumentation, T. Kawata for XRD measurements, and Dr M. Maeda for SEM image acquisitions at N-BARD, Hiroshima University, and S. Watanabe and M. Yoshimi for XPS measurements in the Shimadzu Corporation. Funding in the form of a grant from the Japan Society for the Promotion of Science (Next Generation World-Leading Researchers program, GR073), a Grant-in-Aid for Scientific Research (A) (15H02001), Grants-in-Aid for Scientific Research (B) (19H02556 and 22H01909), and a Grant-in-Aid for Challenging Research (Pioneering) (23K17348) are acknowledged, as well as funding from the Japan Science and Technology Agency (JST) for PRESTO (Structure Control and Function program) and from the JKA (2019-M188 and 2023-M418).

References

1 J. A. Turner, *Science*, 2004, **305**, 972–974.
2 I. Staffell, D. Scamman, A. Velazquez Abad, P. Balcombe, P. E. Dodds, P. Ekins, N. Shah and K. R. Ward, *Energy Environ. Sci.*, 2019, **12**, 463–491.
3 R. Chaubey, S. Sahu, O. O. James and S. Maity, *Renew. Sustain. Energy Rev.*, 2013, **23**, 443–462.
4 K. Zeng and D. Zhang, *Prog. Energy Combust. Sci.*, 2010, **36**, 307–326.
5 M. A. Khan, T. Al-Attas, S. Roy, M. M. Rahman, N. Ghaffour, V. Thangadurai, S. Larter, J. Hu, P. M. Ajayan and Md. G. Kibria, *Energy Environ. Sci.*, 2021, **14**, 4831–4839.
6 X. Zou and Y. Zhang, *Chem. Soc. Rev.*, 2015, **44**, 5148–5180.
7 Y. Zhu, Q. Lin, Y. Zhong, H. A. Tahini, Z. Shao and H. Wang, *Energy Environ. Sci.*, 2020, **13**, 3361–3392.
8 A. Steinfeld, *Sol. Energy*, 2005, **78**, 603–615.
9 B. Xu, Y. Bhawe and M. E. Davis, *Proc. Natl. Acad. Sci. U. S. A.*, 2012, **109**, 9260–9264.
10 S. Dutta, *Energy Fuels*, 2021, **35**, 11613–11639.
11 P. V. Kamat and K. Sivula, *ACS Energy Lett.*, 2022, **7**, 3149–3150.
12 R. D. Cortright, R. R. Davda and J. A. Dumesic, *Nature*, 2002, **418**, 964–967.
13 Y. Guo, S. Z. Wang, D. H. Xu, Y. M. Gong, H. H. Ma and X. Y. Tang, *Renew. Sustain. Energy Rev.*, 2010, **14**, 334–343.
14 X. Zhu, Q. Imtiaz, F. Donat, C. R. Müller and F. Li, *Energy Environ. Sci.*, 2020, **13**, 772–804.
15 L. Zeng, Z. Cheng, J. A. Fan, L.-S. Fan and J. Gong, *Nat. Rev. Chem.*, 2018, **2**, 349–364.
16 Z. Zhao, M. Uddi, N. Tsvetkov, B. Yildiz and A. F. Ghoniem, *J. Phys. Chem. C*, 2016, **120**, 16271–16289.
17 S. Xu, X. Zhao and J. Liu, *Renew. Sustain. Energy Rev.*, 2018, **92**, 17–37.
18 M. Esmaily, J. E. Svensson, S. Fajardo, N. Birbilis, G. S. Frankel, S. Virtanen, R. Arrabal, S. Thomas and L. G. Johansson, *Prog. Mater. Sci.*, 2017, **89**, 92–193.
19 H. Z. Wang, D. Y. C. Leung, M. K. H. Leung and M. Ni, *Renew. Sustain. Energy Rev.*, 2009, **13**, 845–853.
20 X. Huang, T. Gao, X. Pan, D. Wei, C. Lv, L. Qin and Y. Huang, *J. Power Sources*, 2013, **229**, 133–140.
21 T. Friščić, C. Mottillo and H. M. Titi, *Angew. Chem., Int. Ed.*, 2020, **59**, 1018–1029.
22 Y. Wang and K. Saitow, *Chem. Mater.*, 2020, **32**, 9190–9200.
23 Y. Miura, T. Kashiwagi, T. Fukuda, A. Shichiri, T. Shiobara and K. Saitow, *ACS Sustain. Chem. Eng.*, 2022, **10**, 16159–16168.
24 A. P. Amrute, Z. Łodziana, H. Schreyer, C. Weidenthaler and F. Schüth, *Science*, 2019, **366**, 485–489.
25 H. Murata, Y. Kataoka, T. Kawamoto, I. Tanaka and T. Taniguchi, *Phys. Status Solidi RRL*, 2014, **8**, 822–826.
26 A. El Goresy, M. Chen, P. Gillet, L. Dubrovinsky, G. Graup and R. Ahuja, *Earth Planet. Sci. Lett.*, 2001, **192**, 485–495.
27 K. Domen, J. N. Kondo, M. Hara and T. Takata, *Bull. Chem. Soc. Jpn.*, 2000, **73**, 1307–1331.
28 F. Delogu, *Int. J. Hydrog. Energy*, 2011, **36**, 15145–15152.
29 Y. Sawama, M. Niikawa, Y. Yabe, R. Goto, T. Kawajiri, T. Marumoto, T. Takahashi, M. Itoh, Y. Kimura, Y. Sasai, Y. Yamauchi, S. Kondo, M. Kuzuya, Y. Monguchi and H. Sajiki, *ACS Sustainable Chem. Eng.*, 2015, **3**, 683–689.
30 K. Saitow and T. Wakamiya, *Appl. Phys. Lett.*, 2013, **103**, 031916.
31 T. Mizutani, H. Ohta, T. Ueda, T. Kashiwagi, T. Fukuda, T. Shiobara and K. Saitow, *ACS Sustainable Chem. Eng.*, 2023, **11**, 11769–11780.
32 K. Saitow, Y. Wang and S. Takahashi, *Sci. Rep.*, 2018, **8**, 15549.
33 K. Yoshihara, M. Sakamoto, H. Tamamitsu, M. Arakawa and K. Saitow, *Adv. Opt. Mater.*, 2018, **6**, 1800462.
34 H. Sun, S. Miyazaki, H. Tamamitsu and K. Saitow, *Chem. Commun.*, 2013, **49**, 10302–10304.
35 G. Z. Chen, D. J. Fray and T. W. Farthing, *Metall. Mater. Trans. B*, 2001, **32**, 1041–1052.

36 W. Pickhardt, S. Grätz and L. Borchardt, *Chemistry*, 2020, **26**, 12903–12911.
37 P. Atkins and J. de Paula, *Physical Chemistry*, Oxford University Press, 10th edn, 2014.
38 A. Steinfeld, P. Kuhn, A. Reller, R. Palumbo, J. Murray and Y. Tamaura, *Int. J. Hydrogen Energy*, 1998, **23**, 767–774.
39 Q. Bignon, F. Martin, Q. Auzoux, F. Miserque, M. Tabarant, L. Latu-Romain and Y. Wouters, *Corros. Sci.*, 2019, **150**, 32–41.
40 J. Paier, C. Penschke and J. Sauer, *Chem. Rev.*, 2013, **113**, 3949–3985.
41 U. Diebold, *Surf. Sci. Rep.*, 2003, **48**, 53–229.
42 F. K. Urakaev and V. V. Boldyrev, *Powder Technol.*, 2000, **107**, 93–107.
43 F. K. Urakaev, in *Mechanochemical Processing of Nanopowders*, ed. M. Sopicka-Lizer, Woodhead Publishing, 1st edn, 2010, ch. 2, pp. 9–44.
44 S. R. Chauruka, A. Hassanpour, R. Brydson, K. J. Roberts, M. Ghadiri and H. Stitt, *Chem. Eng. Sci.*, 2015, **134**, 774–783.
45 S. Bégin-Colin, T. Girot, G. L. Le Caër and A. Mocellin, *J. Solid State Chem.*, 2000, **149**, 41–48.
46 A. Naldoni, M. Altomare, G. Zoppellaro, N. Liu, Š. Kment, R. Zbořil and P. Schmuki, *ACS Catal.*, 2019, **9**, 345–364.
47 X. Tang, S. Wang, L. Qian, Y. Li, Z. Lin, D. Xu and Y. zhang, *Chem. Eng. Res. Des.*, 2015, **100**, 530–541.
48 T. Morita, K. Kusano, H. Ochiai, K. Saitow and K. Nishikawa, *J. Chem. Phys.*, 2000, **112**, 4203–4211.
49 K. A. Trowell, S. Goroshin, D. L. Frost and J. M. Bergthorson, *Sustain. Energy Fuels*, 2020, **4**, 5628–5635.
50 A. Kruse and E. Dinjus, *Angew. Chem., Int. Ed.*, 2003, **42**, 909–911.
51 J. Hidalgo-Jiménez, T. Akbay, T. Ishihara and K. Edalati, *J. Mater. Chem. A*, 2023, **11**, 23523–23535.
52 A. Navrotsky, L. Mazeina and J. Majzlan, *Science*, 2008, **319**, 1635–1638.
53 A. Navrotsky, *ChemPhysChem*, 2011, **12**, 2207–2215.
54 A. M. Belenguer, G. I. Lampronti, A. J. Cruz-Cabeza, C. A. Hunter and J. K. M. Sanders, *Chem. Sci.*, 2016, **7**, 6617–6627.
55 S. Mateti, M. Mathesh, Z. Liu, T. Tao, T. Ramireddy, A. M. Glushenkov, W. Yang and Y. I. Chen, *Chem. Commun.*, 2021, **57**, 1080–1092.
56 **https://www.nrel.gov/csp/generation-3-concentrating-solar-power-systems.html**, accessed 2024-09-27.
57 L. A. Weinstein, J. Loomis, B. Bhatia, D. M. Bierman, E. N. Wang and G. Chen, *Chem. Rev.*, 2015, **115**, 12797–12838.
58 A. A. L. Michalchuk and F. Emmerling, *Angew. Chem., Int. Ed.*, 2022, **61**, e202117270.
59 T. Friščić, I. Halasz, P. J. Beldon, A. M. Belenguer, F. Adams, S. A. J. Kimber, V. Honkimäki and R. E. Dinnebier, *Nat. Chem.*, 2013, **5**, 66–73.